Alma Mater Studiorum · Università di Bologna

Scuola di Scienze
Dipartimento di Fisica e Astronomia
Corso di Laurea in Fisica

Synchronization of coupled oscillators

Relatore:
Prof. Armando Bazzani

Correlatore:
Dott. Federico Capoani

Presentata da:
Lorenzo Mensi

Anno Accademico 2022/2023

Abstract

Synchronization is ubiquitous in nature. Indeed, periodic phenomena with similar frequencies have been observed to synchronize their phases during their evolution. From a mathematical point of view it can be defined as the tendency of coupled periodic systems to reach a point of equilibrium characterized by a relative phase equal to a multiple integer of 2π (in-phase oscillations) or to an odd integer of π (anti-phase oscillations). In this report we analyzed this phenomenon using two different dynamical systems coupled via a trolley: one built with simple pendulums, where oscillations are damped by friction, and the other built with metronomes, where a spring supplies energy to the oscillating mass to compensate dissipative effects. In each system both in-phase and anti-phase synchronization have been observed by varying the initial conditions. By building the systems and employing both an analytical and numerical model in order to understand experimental data, the primary causes of the synchronization phenomenon can be linked to the variation of energy, and consequently to dissipation and energy supplied by the spring.

La sincronizzazione è onnipresente in natura. Infatti, si osserva che fenomeni periodici con frequenze simili sincronizzano le loro fasi durante la loro evoluzione. Da un punto di vista matematico puó essere definita come la tendenza di sistemi periodici in interazione tra loro a raggiungere uno stato di equilibrio caratterizzato da una fase relativa pari ad un multiplo intero di 2π (oscillazioni in fase) oppure un multiplo dispari di π (oscillazioni in controfase). In questa tesi viene studiato il fenomeno della sincronizzazione per due diversi sistemi di oscillatori accoppiati mediante un carrellino; il primo costituito da due pendoli semplici, soggetti all'attrito, e il secondo da due metronomi, in cui la dissipazione viene compensata da una molla che fornisce energia alla massa oscillante. Sia lo stato sincrono in fase che in controfase sono stati osservati sperimentalmente in entrambi i sistemi, in base alle condizioni iniziali. Utilizzando un approccio analitico, sperimentale e numerico, le cause che portano alla sincronizzazione sono state ricondotte alla variazione di energia, ovvero alla dissipazione dell'attrito e all'energia immessa dalla molla.

Contents

Introduction

Physics of Complex Systems is the study of systems composed by many components and considers the peculiar global properties which emerge from the interactions between subsystems. Examples of systems where the whole is greater than the sum of its parts can be found in many fields, such as neuroscience [1], Earth sciences [2], economics [3], city planning [4] and many more. An instance of a non trivial property which stems from interaction is synchronization; a complex system is in a synchronous state when a specific phenomenon occurs at the same time in every subsystem.
The phenomenon of synchronization is not uncommon in biological systems, and in certain cases it is a crucial mechanism employed to ensure the correct functioning of important organs, such as hearts, were coupled pacemaker cells act in synchronous fashion [5]. Sometimes the reason beyond synchronization is more mysterious and might be linked to evolutionary advantages: certain species of fireflies have been seen blinking in unison, turning pitch black nights into beautiful light shows [6].
The most successful approach to study synchronous behaviour in these types of systems, was introduced by Kuramoto [7], who proposed a non-linear model which can be solved analytically, even in the limit of infinite oscillators. The strength of the model lies in its ability to describe huge networks of oscillators, and their eventual evolution towards synchronous states.
Christiaan Huygens (1629-1695) was the first to observe and describe synchronous behaviour in pendulum clocks [8], which were invented by him. By hanging two identical clocks to the same support beam, the pendulums could interact with each other by exchanging momentum, meaning that the dynamic of each clock was influenced by the behaviour of the other, hence the two oscillators were *coupled*. Although the clocks were put in motion with different phases, the "ticks" eventually occurred at the same time, as the pendulums swung in synchronous motion, with opposite angular velocities. We decided to follow Huygens' steps and study two different types of systems of physical oscillators, one built using pendulums and the other made with metronomes. These systems are comprised of two oscillators each, and the aim of this report is to experimentally verify the stability of synchronous motion and to create a linear model which predicts the final state.
A system of coupled oscillators can be easily built by attaching two pendulums to the

same trolley: due to the law of conservation of momentum, the swings of a pendulum cause the cart to move, thus influencing the dynamic of the other pendulum; since each oscillator interacts with the other, they are coupled. A point of equilibrium is reached when *phase locking* occurs, a state in which each oscillator can be mathematically modelled as a time dependent periodic function with a constant phase. When the relative phase difference between the oscillators is a multiple integer of 2π or an odd integer of π the system has reached a *synchronized* state; in the first case the oscillations occur *in-phase* while in the other in *anti-phase*. When perfect in-phase synchronization occurs, the pendulums swing together and the motion of the trolley is maximized, while in the case of perfect anti-phase the pendulums have opposite angular velocities, hence the cart does not move at all and the pendulums behave as if they were uncoupled. In recent years, an analogous system built using metronomes [9] has been popularized by online videos: the key difference between a pendulum and a metronome is that in the former case oscillations are damped by friction, while in the latter a spring injects energy into the oscillating mass, increasing its angular velocity, thus compensating friction and sustaining the oscillations.

This thesis contains the results of experiments we performed, verifying the conditions for the existence of synchronized states and that different synchronous stationary states are possible depending on the initial conditions. In Chapter 1 we explore in detail the theoretical analysis of both systems, and mathematically explain how synchronization is linked to the variation of energy, caused either by friction or by the spring's action on the swinging mass. In Chapter 2 we report data which we gathered by building the setups and by carrying out frame by frame video analysis of the dynamical evolution of these systems. Finally, in Chapter 3 we present numerical solutions to the equations of motion, as well as some modifications to the model which can be made to more accurately reproduce real world data.

Chapter 1

Theoretical analysis

1.1 Coupled pendulums

A system of oscillators is said to be coupled if the dynamic of a single member is influenced by the behaviour of all the others. The simplest system of this kind is one comprised of the most well known oscillators: pendulums.

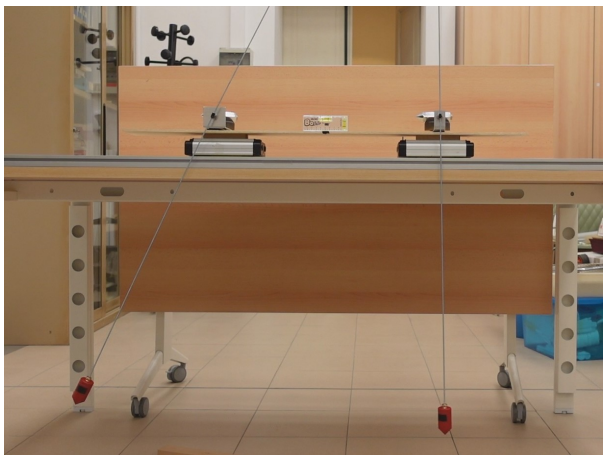

Figure 1.1: *Example of coupled pendulums. The system can be mathematically modeled by using the position of the trolley's center and the angle between the oscillating masses and the vertical.*

Consider two point mass pendulums of length l and mass m pivoted on the same cart of mass M (Fig. 1.1), which can move on a straight line along the x axis, dragging the pendulums' pivot points. As the pendulums swing around their respective resting point, the cart moves, since the x component of momentum is conserved. The horizontal velocity of each pendulum can be written as $\dot{x}_i = \dot{X} + l\cos(\theta_i)\dot{\theta}_i$, where X is the position

of the center of the cart and θ is the angle between the oscillating mass and its point of equilibrium; therefore the relation which defines the conservation of momentum is

$$M\dot{X} + m(\dot{X} + l\cos(\theta_1)\dot{\theta_1}) + m(\dot{X} + l\cos(\theta_2)\dot{\theta_2}) = 0$$

which yields an equation for $\dot{X}$

$$\dot{X} = -\frac{m}{2m+M} l(\cos(\theta_1)\dot{\theta_1} + \cos(\theta_2)\dot{\theta_2}) = -al(\cos(\theta_1)\dot{\theta_1} + \cos(\theta_2)\dot{\theta_2}) \tag{1.1}$$

where $a = m/(2m+M)$ can be related to the effectiveness of coupling: a super massive cart would not be affected by the motion of the swinging masses and would remain stationary, consequently preventing the oscillators from interacting (for $M \to +\infty$, $a \to 0$), while a lighter cart would cause the dynamic of each pendulum to be greatly influenced by the motion of the other (for $M \to 0$, $a \to \frac{1}{2}$) . Using $y_i = l\cos(\theta_i)$, $\dot{y_i} = -l\sin(\theta_i)\dot{\theta_i}$ we can derive the kinetic energy T and potential energy V of the system

$$\begin{aligned} T &= \frac{M}{2}\dot{X}^2 + \frac{m}{2}(\dot{x_1}^2 + \dot{y_1}^2) + \frac{m}{2}(\dot{x_2}^2 + \dot{y_2}^2) = \\ &= \left(\frac{M}{2} + m\right)\dot{X}^2 + m\dot{X}l(\cos(\theta_1)\dot{\theta_1} + \cos(\theta_2)\dot{\theta_2}) + \frac{m}{2}l^2(\dot{\theta_1}^2 + \dot{\theta_2}^2) \end{aligned}$$

By substituting $\dot{X}$ with the expression given by Eq. 1.1, the energy of the system can be expressed solely as a function of the angular positions θ_i

$$\begin{aligned} T &= \frac{m}{2}l^2(\dot{\theta_1}^2 + \dot{\theta_2}^2) + ma(a + a\frac{M}{2m} - 1)l^2(\cos(\theta_1)\dot{\theta_1} + \cos(\theta_2)\dot{\theta_2})^2 = \\ &= \frac{m}{2}l^2(\dot{\theta_1}^2 + \dot{\theta_2}^2) - ml^2\frac{a}{2}(\cos(\theta_1)\dot{\theta_1} + \cos(\theta_2)\dot{\theta_2})^2 \\ V &= mgl(2 - \cos(\theta_1) - \cos(\theta_2)) \end{aligned}$$

where g is the acceleration due to gravity. To simplify these relations, one can adopt a second order small angle approximation, which is fairly accurate as long as $\theta_i < \pi/6$. By assuming $\sin(\theta_i) \approx \theta_i$ and $\cos(\theta_i) \approx\ 1 - \theta_i^2/2$ an approximate form of the total energy of the system can be obtained

$$E = T + V = l^2\frac{m}{2}(\dot{\theta_1}^2 + \dot{\theta_2}^2) - ml^2\frac{a}{2}\left[\left(1 - \frac{\theta_1^2}{2}\right)\dot{\theta_1} + \left(1 - \frac{\theta_2^2}{2}\right)\dot{\theta_2}\right]^2 + \frac{mgl}{2}(\theta_1^2 + \theta_2^2) \tag{1.2}$$

For the sake of simplicity, let us consider the limit of low angular velocities, and treat $\dot{\theta_i}$ as a term of the same order of magnitude of θ_i. In general this is not true, but it should be justified as long as low enough frequencies are considered. The implications of

this approximation will be further explored in the following sections and are confirmed a posteriori by experimental data (Sect. 2.2). When the approximation holds, the product $\theta_i^2\dot{\theta}_i$ is of the third order and therefore the energy can be rewritten as

$$T = \frac{ml^2}{4}[(\dot{\theta}_1 + \dot{\theta}_2)^2 + (\dot{\theta}_1 - \dot{\theta}_2)^2] - \frac{mal^2}{2}(\dot{\theta}_1 + \dot{\theta}_2)^2 \tag{1.3}$$

$$V = \frac{mgl}{4}[(\theta_1 + \theta_2)^2 + (\theta_1 - \theta_2)^2] \tag{1.4}$$

The phenomenon of synchronization can be nimbly studied by introducing two new variables, $d = \theta_1 - \theta_2$ and $s = \theta_1 + \theta_2$. These variables grant meaningful insight on the state of the system, as in-phase motion is characterized by $d = 0$, while an identically null value of s is typical of anti-phase synchronization. The equations of motion can be cast as a function of s and d, and are easily obtained by using the Lagrangian:

$$\ddot{d} + \omega^2 d = 0 \tag{1.5}$$

$$(1 - 2a)\ddot{s} + \omega^2 s = 0 \tag{1.6}$$

where $\omega^2 = g/l$. These equations describe a periodic dynamic of d and s with respective angular frequency ω and $\omega/\sqrt{1-2a}$; they also provide an effective way to study the evolution of the system, as they are uncoupled and can be studied separately. A synchronous state is achieved when either s or d is identically null while the other variable is described by a periodic function, hence in this case, where energy is conserved and the dynamic is described by uncoupled equations, no synchronization can occur.
However, the real-world system is not accurately modeled by this approach, as it is subject to friction, which causes energy to vary; this key effect needs to be introduced into the equations of motion as it is crucial to the study of synchronization.
The simplest way to model friction is by introducing a new term to the differential equations which is proportional to the angular velocity and a constant, γ, with the dimensions of a frequency. The underlying assumption here is that the dominant dissipative effect is the one acting on the pivot, thus mainly affecting the rotational dynamic of the swinging masses by damping oscillations. As long as all the aforementioned approximations are valid, the system is described by the following coupled equations

$$\ddot{\theta}_1 + \gamma\dot{\theta}_1 + \omega^2\theta_1 - a(\ddot{\theta}_1 + \ddot{\theta}_2) = 0 \tag{1.7}$$
$$\ddot{\theta}_2 + \gamma\dot{\theta}_2 + \omega^2\theta_2 - a(\ddot{\theta}_1 + \ddot{\theta}_2) = 0 \tag{1.8}$$

which can be uncoupled by using the variables d and s

$$\ddot{d} + \gamma\dot{d} + \omega^2 d = 0 \tag{1.9}$$
$$(1 - 2a)\ddot{s} + \gamma\dot{s} + \omega^2 s = 0 \tag{1.10}$$

It is convenient to substitute the parameter γ with γ_d in Eq. 1.9 and $\gamma/(1-2a)$ with γ_s in Eq. 1.10 in order to account for the more general case, where other dissipative effects, which might affect d and s asymmetrically, should be considered. When the conditions $\omega^2 > \gamma_d^2/4, (1-2a)\gamma_s^2/4$ hold the solution to the system can be written as follows:

$$d(t) = \exp\left(-\frac{\gamma_d}{2}t\right)(A_d\cos(\omega_d t) + B_d\sin(\omega_d t)) \tag{1.11}$$

$$s(t) = \exp\left(-\frac{\gamma_s}{2}t\right)(A_s\cos(\omega_s t) + B_s\sin(\omega_s t)) \tag{1.12}$$

where $\omega_d = \sqrt{\omega^2 - \gamma_d^2/4}$, $\omega_s = \sqrt{\omega^2/(1-2a) - \gamma_s^2/4}$ and A_d, B_d, A_s, B_s are determined by the initial condition. Since the exponential factors are different, one solution might be dissipated faster than the other, leading to synchronization. This is the case described by Eqs. 1.9 and 1.10, with $\gamma_d = \gamma$ and $\gamma_s = \gamma/(1-2a)$; a is bound by 0 and 1/2, which implies that the oscillation amplitude of $s(t)$ has an higher decay rate than that of $d(t)$, hence with "fair" starting conditions, where the initial amplitudes A_d, B_d and A_s, B_s are comparable, anti-phase synchronization is favoured.

1.2 Energy of the system

In the case of high angular velocities, the kinetic energy cannot be written as in Eq. 1.3, but, if the small angle approximation is still valid, it can be expressed as

$$\begin{aligned}
T &\approx \frac{m}{2}l^2\left(\dot{\theta_1}^2 + \dot{\theta_2}^2\right) - ml^2\frac{a}{2}\left[\left(1-\frac{\theta_1^2}{2}\right)\dot{\theta}_1 + \left(1-\frac{\theta_2^2}{2}\right)\dot{\theta}_2\right]^2 \\
&\approx \frac{ml^2}{4}\left[(\dot{\theta}_1+\dot{\theta}_2)^2 + (\dot{\theta}_1-\dot{\theta}_2)^2\right] - \frac{mal^2}{2}\left[\left(1-\theta_1^2\right)\dot{\theta_1}^2 + \left(1-\theta_2^2\right)\dot{\theta_2}^2 + 2\left(1-\frac{\theta_1^2+\theta_2^2}{2}\right)\dot{\theta}_1\dot{\theta}_2\right] \\
&= \frac{ml^2}{4}\left[\dot{s}^2 + \dot{d}^2\right] - \frac{mal^2}{2}\left[\dot{\theta_1}^2 + \dot{\theta_2}^2 + 2\dot{\theta}_1\dot{\theta}_2 - \theta_1^2\dot{\theta_1}^2 - \theta_2^2\dot{\theta_2}^2 - (\theta_1^2+\theta_2^2)\dot{\theta}_1\dot{\theta}_2\right]
\end{aligned}$$

which can be rewritten solely as a function of d, s and their time derivatives by making the following considerations:

$$\begin{aligned}
(\theta_1^2+\theta_2^2)\dot{\theta}_1\dot{\theta}_2 &= \frac{1}{2}(s^2+d^2)\frac{1}{4}(\dot{s}^2-\dot{d}^2) \\
&= \frac{1}{8}(s^2\dot{s}^2 - s^2\dot{d}^2 + d^2\dot{s}^2 - d^2\dot{d}^2)
\end{aligned}$$

$$\begin{aligned}\theta_1^2\dot{\theta_1}^2 + \theta_2^2\dot{\theta_2}^2 &= (\theta_1^2+\theta_2^2)\dot{\theta_1}^2 + (\theta_1^2+\theta_2^2)\dot{\theta_2}^2 - \theta_2^2\dot{\theta_1}^2 - \theta_1^2\dot{\theta_2}^2 \\ &= (\theta_1^2+\theta_2^2)(\dot{\theta_1}^2+\dot{\theta_2}^2) + (\theta_1^2-\theta_2^2)\dot{\theta_1}^2 - (\theta_1^2-\theta_2^2)\dot{\theta_2}^2 - \theta_1^2\dot{\theta_1}^2 - \theta_2^2\dot{\theta_2}^2 \\ &= \frac{1}{8}(s^2+d^2)(\dot{s}^2+\dot{d}^2) + \frac{1}{2}sd\dot{s}\dot{d}\end{aligned}$$

and

$$(\theta_1^2+\theta_2^2)\dot{\theta_1}\dot{\theta_2} + \theta_1^2\dot{\theta_1}^2 + \theta_2^2\dot{\theta_2}^2 = \frac{1}{4}\dot{s}^2(s^2+d^2) + \frac{1}{2}sd\dot{s}\dot{d}$$

which implies that $4T/(ml^2) = \dot{s}^2 + \dot{d}^2 - 2a\dot{s}^2 + \frac{a}{2}\dot{s}^2(s^2-d^2) + asd\dot{s}\dot{d}$
Therefore, we obtain an expression for the energy of the system which was derived by only employing the small angle approximation

$$E = \frac{ml^2}{4}\dot{s}^2\Big(1 - 2a + \frac{a}{2}(s^2-d^2)\Big) + \frac{ml^2}{4}\dot{d}^2 + \frac{mal^2}{4}sd\dot{s}\dot{d} + \frac{mgl}{4}(s^2+d^2). \tag{1.13}$$

Unfortunately, the equations of motion yielded by 1.13, which provides a more realistic depiction of the physical reality, have no analytical solutions. Nevertheless, it is possible to identify the corrective terms E_c which are neglected when the small angular velocity approximation is adopted by comparing Eq. 1.13 with Eq. 1.3, thus providing a formal way to evaluate the accuracy of such estimate. We can introduce three new quantities, e_s, e_d and e_c, defined by the following relations

$$e_s = \frac{4E_s}{ml^2} = \dot{s}^2(1-2a) + \omega^2 s^2 \tag{1.14}$$

$$e_d = \frac{4E_d}{ml^2} = \dot{d}^2 + \omega^2 d^2 \tag{1.15}$$

$$e_c = \frac{4E_c}{ml^2} = asd\dot{s}\dot{d} - \frac{a}{2}\dot{s}^2\dot{d}^2 + \frac{a}{2}\dot{s}^2 s^2 \tag{1.16}$$

and claim that the simplified approach is still reasonable as long as $|e_c| \ll e_d, e_s$. If the approximate forms given by 1.11 and 1.12 are still valid to some degree, one can observe that the rate at which e_c is dissipated is equal to $\gamma_d + \gamma_s$, which means that in certain cases the approximation might be valid after a certain period of time, since e_c decays faster than e_s and e_d.
When e_c is negligible, another valid course of action is to express the energy of the system as the sum of the energy contained in the pendulums E_p and the energy of the trolley E_t, which is purely kinetic and defined by the relation $E_t = M\dot{X}^2/2 \approx Ml^2a^2\dot{s}^2/2$. Observing that $Ma = mM/(2m+M) = m(1-2a)$ we derive

$$E_p = T_p + V_p = \frac{ml^2}{4}((1-2a)^2\dot{s}^2 + \dot{d}^2 + \omega^2(s^2+d^2)) \tag{1.17}$$

$$E_t = T_t = \frac{ml^2}{4}2a(1-2a)\dot{s}^2 \tag{1.18}$$

Now that all the relevant physical quantities have been expressed as a function of s d and their time derivatives, we have established a framework which eases the study of synchronization, as it reduces the phenomenon to the evolution of these variables.

1.3 Coupled Metronomes

A metronome can be modelled as a damped harmonic oscillator attached to a spring, which supplies energy to the system in order to sustain the oscillations by compensating dissipation. The stability of synchronous solutions have been the subject of many papers, such as [10]. The effect of the spring can be modelled as an impulsive boost to the magnitude of the oscillating mass' angular velocity: this boost is triggered when the mass reaches its resting position ($\theta = 0$). The equation of motion of an uncoupled metronome can therefore be written using the small angle approximation as

$$\ddot{\theta} + \gamma\dot{\theta} + \omega^2\theta = \mathrm{sgn}(\dot{\theta})K\delta(\theta)$$

where sgn is the sign function, $\delta(\theta)$ is Dirac's delta and K is the angular velocity boost ("kick"). Dirac's delta introduces a discontinuity in the time derivative of θ of magnitude K and sign $\mathrm{sgn}(\dot{\theta})$ when $\theta = 0$. By coupling two identical metronomes using a cart, similarly to what we already discussed with pendulums in Sect. 1.1, we obtain the following equations

$$\begin{aligned}\ddot{\theta}_1 + \gamma\dot{\theta}_1 + \omega^2\theta_1 - a(\ddot{\theta}_1 + \ddot{\theta}_2) &= \mathrm{sgn}(\dot{\theta}_1)K'\delta(\theta_1)\\ \ddot{\theta}_2 + \gamma\dot{\theta}_2 + \omega^2\theta_2 - a(\ddot{\theta}_1 + \ddot{\theta}_2) &= \mathrm{sgn}(\dot{\theta}_2)K'\delta(\theta_2)\end{aligned}$$

where $K' = (1-a)K$ so that the absolute value of the kick is always equal to K. We can now introduce $s = \theta_1 + \theta_2$ and $d = \theta_1 - \theta_2$ in order to rewrite the system as

$$\ddot{s}(1-2a) + \gamma\dot{s} + \omega^2 s = K'[\mathrm{sgn}(\dot{\theta}_1)\delta(\theta_1) + \mathrm{sgn}(\dot{\theta}_2)\delta(\theta_2)] \tag{1.19}$$

$$\ddot{d} + \gamma\dot{d} + \omega^2 d = K'[\mathrm{sgn}(\dot{\theta}_1)\delta(\theta_1) - \mathrm{sgn}(\dot{\theta}_2)\delta(\theta_2)] \tag{1.20}$$

Note that both in-phase (d identically null, $\mathrm{sgn}(\dot{\theta}_1) = \mathrm{sgn}(\dot{\theta}_2)$) and anti-phase ($s$ identically null, $\mathrm{sgn}(\dot{\theta}_1) = -\mathrm{sgn}(\dot{\theta}_2)$) motion are solutions of the system. In general, the final state depends on the initial conditions; in order to show that both states are stable we can study the behaviour of the equations in a neighbourhood of a synchronous solution (either in-phase or anti-phase). Let us hypothesize that the angular position of a metronome can be expressed as a function of the position of the other, $\theta_2(t) = \theta_1(t) - z(t)$, where $|z| \ll |\theta_1|$, so that the system is close to an in-phase synchronous state (the other case is analogous). In order to find an analytical solution, it is convenient to rewrite both Dirac's deltas as a function of time instead of angular position, as the equations

contain time derivatives. This could be done by approximating the dynamic of the first metronome to its uncoupled behaviour, so that the times in which the spring is triggered can be easily computed. Since an ideal uncoupled metronome has a fixed frequency, the position of its oscillating mass can be arbitrarily described as a cosine, and the delta can be rewritten as

$$\delta(\theta_1) \approx \delta(A\cos(\omega t)) = \sum_{n=0}^{+\infty} \delta(t - t_n)$$

where $t_n = \frac{\pi}{2\omega}(2n+1)$ are the instants in which $\cos(\omega t) = 0$. The other delta is triggered when $\theta_2 = 0$, that is when $\theta_1(t) = z(t)$; in virtue of the fact that z is small, the sequence of times $t_{n-\epsilon}$ which solves the latter equation is not that far off from t_n, and can be expressed as $t_{n-\epsilon} = t_n - \epsilon_n$, where ϵ_n is assumed to be a small positive time. Finally, in a neighbourhood of in-phase synchronization the sign of $\dot{\theta_1}$ is the same as $\dot{\theta_2}$, and since we chose to mathematically model θ_1 as a cosine, $\mathrm{sgn}(\dot{\theta_1}(t_n)) = (-1)^{n+1}$. The variables s and d can be expressed as $s = 2\theta_1 - z$ and $d = z$, which implies that Eq. 1.20 can be cast as a function of z.

$$\ddot{z} + \gamma\dot{z} + \omega^2 z = K'(-1)^{n+1} \sum_{n=0}^{+\infty} [\delta(t - t_n) - \delta(t - t_{n-\epsilon})] \tag{1.21}$$

The system can be considered solved once the sequence of ϵ_n is known, as well as the functions z_{n-1}, $z_{n-\epsilon}$ and z_n which satisfy Eq. 1.21 and are respectively defined in the time intervals $]t_{n-1}, t_{n-\epsilon}[$, $]t_{n-\epsilon}, t_n[$ and $]t_n, t_{n+1-\epsilon}[$. A possible solution for the unknown functions z_n which satisfy Eq. 1.21 is

$$z_n = \exp\left(-\frac{\gamma}{2}(t - t_n)\right)[A_n\cos(\omega' t) + B_n\sin(\omega' t)]$$

where $\gamma^2/4 \ll \omega^2$ and $\omega' = \sqrt{\omega^2 - \gamma^2/4} \approx \omega$. The presence of Dirac's deltas imply the following conditions:

$$\begin{aligned} z_{n-1}(t = t_{n-\epsilon}) &= z_{n-\epsilon}(t = t_{n-\epsilon}) \\ \dot{z}_{n-\epsilon}(t = t_{n-\epsilon}) - \dot{z}_{n-1}(t = t_{n-\epsilon}) &= -(-1)^{n+1}K \\ z_n(t = t_n) &= z_{n-\epsilon}(t = t_n) \\ \dot{z_n}(t = t_n) - \dot{z}_{n-\epsilon}(t = t_n) &= (-1)^{n+1}K \end{aligned}$$

By noticing that

$$\begin{aligned} t_n - t_{n-1} &= \frac{\pi}{\omega} \\ \cos(\omega(t_n - \epsilon_n)) &= \cos(\omega t_n)\cos(\omega\epsilon_n) + \sin(\omega t_n)\sin(\omega\epsilon_n) \approx (-1)^n\omega\epsilon_n + o(\epsilon_n^3) \\ \sin(\omega(t_n - \epsilon_n)) &= \sin(\omega t_n)\cos(\omega\epsilon_n) - \cos(\omega t_n)\sin(\omega\epsilon_n) \approx (-1)^n + o(\epsilon_n^2) \end{aligned}$$

and expressing the time derivative of z_n in the convenient form

$$\dot{z}_n = -\frac{\gamma}{2} z_n - \omega \exp\Big(-\frac{\gamma}{2}(t - t_n)\Big)[A_n \sin(\omega t) - B_n \cos(\omega t)]$$

the first two conditions yield the following equations

$$A_{n-\epsilon} = \exp\Big(-\frac{\gamma}{2}(\frac{\pi}{\omega} - \epsilon_n)\Big) A_{n-1} - \frac{K}{\omega} + o(\epsilon_n^2) \tag{1.22}$$

$$B_{n-\epsilon} = \exp\Big(-\frac{\gamma}{2}(\frac{\pi}{\omega} - \epsilon_n)\Big) B_{n-1} + K\epsilon_n + o(\epsilon_n^2) \tag{1.23}$$

Using the remaining conditions, we can express A_n and B_n as a function of A_{n-1} and B_{n-1}

$$A_n = \exp\Big(-\frac{\gamma}{2}\epsilon_n\Big) A_{n-\epsilon} + \frac{K}{\omega} \approx \exp\Big(-\frac{\gamma}{2}\frac{\pi}{\omega}\Big) A_{n-1} + \frac{\gamma}{2}\epsilon_n \frac{K}{\omega} + o(\epsilon_n^2) \tag{1.24}$$

$$B_n = \exp\Big(-\frac{\gamma}{2}\epsilon_n\Big) B_{n-\epsilon} \approx \exp\Big(-\frac{\gamma}{2}\frac{\pi}{\omega}\Big) B_{n-1} + K\epsilon_n + o(\epsilon_n^2) \tag{1.25}$$

$t_{n+1-\epsilon} = t_{n+1} - \epsilon_{n+1}$ is defined as the solution to the equation $\theta_1(t) = z_n(t)$ which implies that

$$A\cos(\omega t_{n+1-\epsilon}) = z_n(t_{n+1-\epsilon})$$

$$A(-1)^{n+1}\omega\epsilon_{n+1} \approx \exp\Big(-\frac{\gamma}{2}\frac{\pi}{\omega}\Big)(1 + \frac{\gamma}{2}\epsilon_{n+1})[A_n(-1)^{n+1}\omega\epsilon_{n+1} + B_n(-1)^{n+1}]$$

$$\epsilon_{n+1} = \frac{B_n}{A\omega \exp\Big(\frac{\gamma}{2}\frac{\pi}{\omega}\Big) - \omega A_n - \frac{\gamma}{2}B_n} \tag{1.26}$$

By knowing z and $\dot{z}$ at a given time we can compute A_{n-1}, B_{n-1}, ϵ_n and solve the problem. Note that under the condition $K\epsilon_n < \frac{\gamma}{2}\frac{\pi}{\omega}B_{n-1}$, $B_n < B_{n-1}$, which indicates that $\epsilon_{n+1} < \epsilon_n$ ($A \gg A_n, B_n$). The sequence of A_n, B_n and ϵ_n reaches 0 for $n \to +\infty$ which entails that z_n eventually becomes identically vanishing, hence in-phase synchronization occurs.

1.4 Estimate of the kick value K

As we have shown in the previous section, the increase in the modulus of the angular velocity K caused by the action of the spring on the oscillating mass is an important parameter of the model, and it is crucial to know its value when comparing theoretical predictions to experimental data. K can be easily computed once the elastic constant of the spring is know; unfortunately it is likely that the latter will not be provided by the manufacturer, and measuring it directly would require a disassembly of the metronome, thus risking to damage the mechanism. One way to estimate the value of the kick is

to assume that the energy supplied by the spring is equal to the energy dissipated by friction, so that the oscillations are sustained. The value of the dissipation factor γ can be measured by unwinding the spring, so that the metronome can be thought as a simple uncoupled pendulum, and the rate at which the amplitude of the oscillations decays can be obtained by studying the dynamic. By letting the oscillating mass fall from a certain height, the trajectory of the pendulum can be described approximately as $\theta(t) = A\exp(-\gamma t/2)\cos(\omega t)$, as long as $\omega^2 \gg \gamma^2/4$, and its energy on average decays as $mglA^2\exp(-\gamma t)/2$. The energy supplied by the spring E_s must be equal to the energy dissipated in half a period, since the spring is triggered twice a period, when $\theta = 0$ and $t = (2n+1)\pi/(2\omega)$; we therefore derive

$$E_s = E(0) - E(\pi/\omega) = \frac{mgl}{2}A^2\Big[1 - \exp\Big(-\gamma\frac{\pi}{\omega}\Big)\Big] \approx \frac{mgl}{2}A^2\frac{\gamma\pi}{\omega} \tag{1.27}$$

The energy immediately after the spring's boost, E_b, can be expressed as $E_b = E(\pi/(2\omega))+ E_s$. Since the energy at a quarter of a period is purely kinetic, the previous expression can be written as $\dot\theta_b^2 = \dot\theta(\pi/(2\omega))^2 + 2E_s/(ml^2)$, where $\dot\theta_b$ is the boosted angular speed; this allows us to compute the value of the kick $K = |\dot\theta_b - \dot\theta(\pi/(2\omega))|$. If we assume that the boost is relatively small, which is coherent with the condition $\omega^2 \gg \gamma^2/4$, we can write $\dot\theta_b^2 - \dot\theta(\frac{\pi}{2\omega})^2 = (\dot\theta_b - \dot\theta(\frac{\pi}{2\omega}))(\dot\theta_b + \dot\theta(\frac{\pi}{2\omega})) \approx K2|\dot\theta(\frac{\pi}{2\omega})|$ which means that $K = E_s/(ml^2|\dot\theta(\frac{\pi}{2\omega})|)$. By using Eq. 1.27, $\omega^2 = g/l$ and $|\dot\theta(\pi/(2\omega))| = \omega A\exp\Big(-\frac{\gamma}{2}\frac{\pi}{2\omega}\Big)$ the previous expression can be written as

$$K = \frac{\gamma\pi A}{2}\exp\Big(\frac{\gamma}{2}\frac{\pi}{2\omega}\Big) \approx \frac{\gamma\pi A}{2}\Big(1 + \frac{\gamma\pi}{4\omega}\Big) \tag{1.28}$$

The energy boost provided by the spring can be clearly seen when plotting the energy of the system as a function of time; as it is shown in Fig. 2.9, the assumption that the "kick" is instantaneous holds. Another effect exhibited by Eq. 1.27 is that at higher angular frequencies oscillations occur with higher amplitudes; $E_s = mg^2\gamma\pi A^2/(2\omega^3)$, which means that if the energy supplied by the spring and γ do not change with the frequency (as in standard metronomes) A^2/ω^3 is constant. An high oscillation amplitude reduces the effectiveness of the model as it is largely based on the small angle approximation. For this reason, a numerical study of the equations obtained in the previous paragraphs is provided in Chapter 3.

Chapter 2

Experimental Setup and Results

2.1 Experimental Setup and Trajectory Tracking

(a) *Coupled Pendulums*

(b) *Coupled Metronomes*

Figure 2.1: *The setups used in the experiment.*

In order to verify the validity of the model studied in the previous sections, we decided to build both systems, one with pendulums and the other with metronomes, to provide evidence that synchronization does indeed occur. The first system (Fig. 2.1a) has been built using two identical plumb-line weights with a mass $m = 280\,\mathrm{g}$, connected to a low-friction trolley ($M = 2500\,\mathrm{g}$) via an unextendable metal rod of adjustable length, thus achieving a system of coupled pendulums characterized by a value of $a = m/(2m + M) \approx 0.09$. The second setup is comprised of Martisan NM-20 mechanical metronomes, which were chosen for their competitive price. Unfortunately, for this system we could not use the

same cart, since it is quite massive and the oscillating mass of the metronome is already much lighter than the weight of its base, meaning that the value of a, hence the effectiveness of coupling, would have been minuscule. In order to maximize the interaction between the oscillators we had to rely on more rudimentary options, which yield higher values of a, by employing a cardboard as a base and tennis balls or cans as wheels (Fig. 2.1b). We could not measure the value of the oscillating mass without damaging the integrity of the metronome, so we obtained the parameter $a \approx 0.02$ through a fit, by tracking the position X of the center of the trolley and using Eq. 1.1. While crafty solutions had to be adopted, synchronization still occurs and the setup is easily reproducible without having access to an extensive budget.

An accurate way to gather data on the trajectories of the oscillating masses is to perform frame-by-frame analysis of videos of the system. In order to do so, we used a simple open-source program called "Tracker" [11] (see Fig. 2.2), which allowed to easily obtain the angular positions θ_1, θ_2 by changing the frame of reference to the correct pivot point. By knowing the frame-rate of the videos, which were usually shot at 50 frames per second, we were also able to compute the angular velocities using the formula $\dot{\theta}_i(t) = (\theta_i(t+\Delta t) - \theta_i(t))/\Delta t$, where Δt is the reciprocal of the frame rate. Unfortunately, this software does not provide standard guidelines on how to estimate uncertainties as there are many effects to take into account: trajectory detection is less precise around the points of maximum velocity, as motion blur is stronger, causing the program to sometimes lose its reference point and requiring manual assistance. This effect can be reduced by shooting at higher shutter speeds, but loss of auto-tracking still occurs, rendering an objective evaluation of uncertainties arduous.

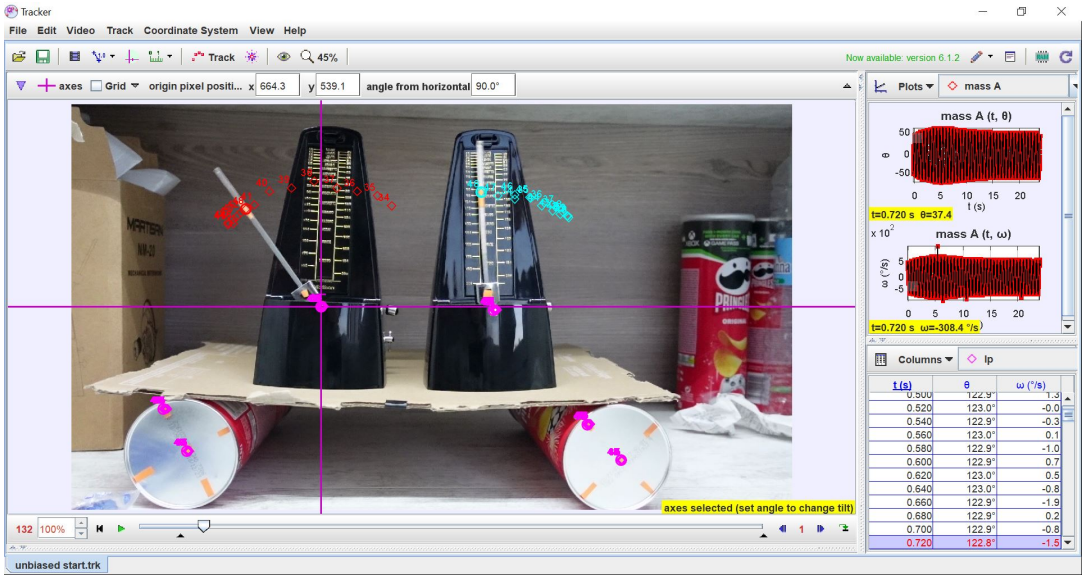

Figure 2.2: *Interface of "Tracker", the program used for tracking trajectories. In this case the wheels were also tracked with the objective of reconstructing the dynamic of the trolley and obtaining an estimate of the value of a.*

2.2 Pendulums: Experimental Data

In the system built using pendulums both synchronized states have been experimentally observed, but in-phase synchronization only occurred with special initial conditions while the system generally seemed to evolve towards anti-phase synchronization. Referring to Eq. 1.11 and 1.12, "fair" starting conditions can be achieved by leaving a pendulum in its resting state and dropping the other from a certain altitude, so that $|s(0)| = |d(0)|$ and $A_d = A_s, B_d = B_s = 0$, as can be seen in the video of Ref. [12].

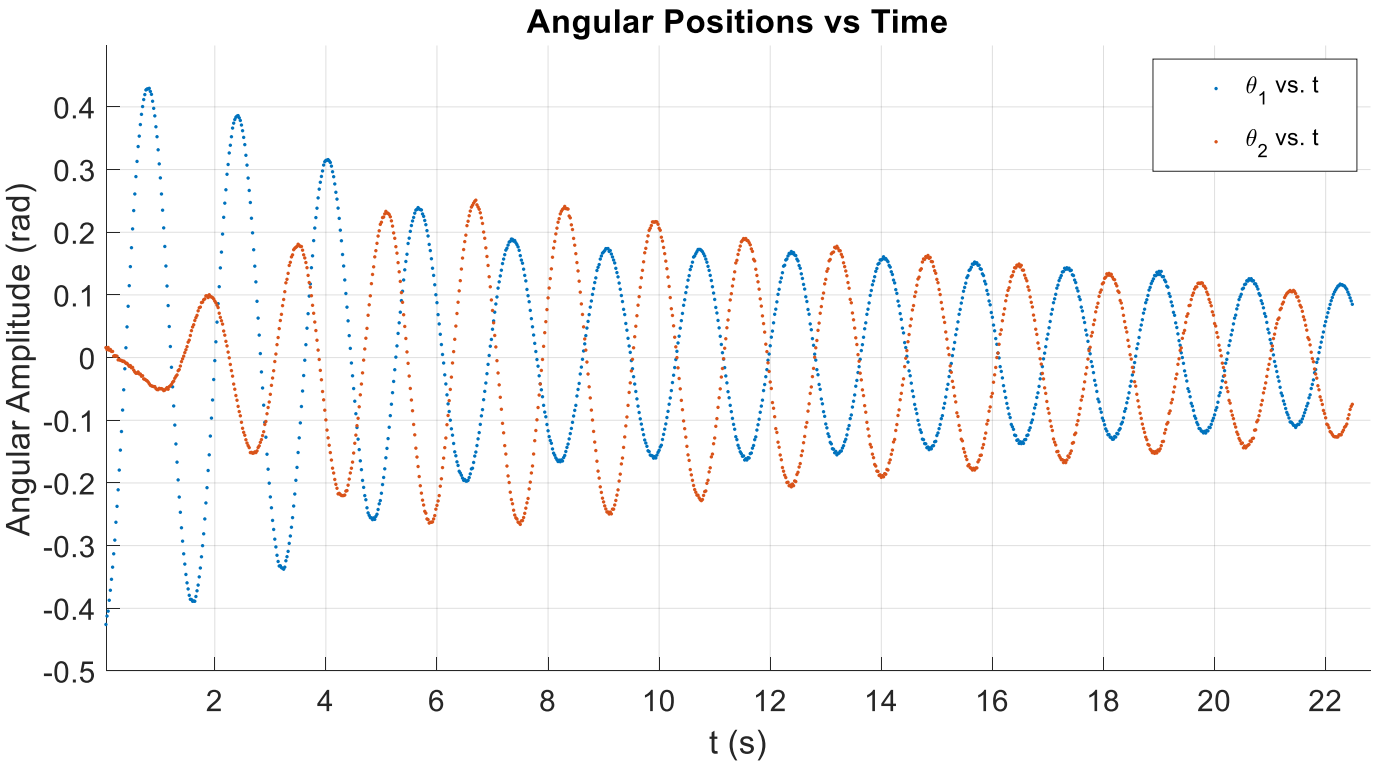

Figure 2.3: *Plot of the experimental data of θ_1 (blue) and θ_2 (red) as a function of time. One pendulum was left in its resting position, while the other was dropped from a certain height, thus achieving an "unbiased" start. Anti-phase synchronization occurs after approximately 10 seconds and lasts until the whole energy of the system is dissipated by friction and the pendulums stop swinging.*

The only configuration in which in-phase motion was observed is when the pendulums were started with a strong bias towards phase synchronization, hence $A_s, B_s \gg A_d, B_d$. The easiest way to achieve such state was to act on the cart, by forcing it to move with a frequency close to $\omega/\sqrt{1-2a}$, thus inducing in-phase motion [13]. The time evolution of s in this configuration is shown in Fig. 2.4

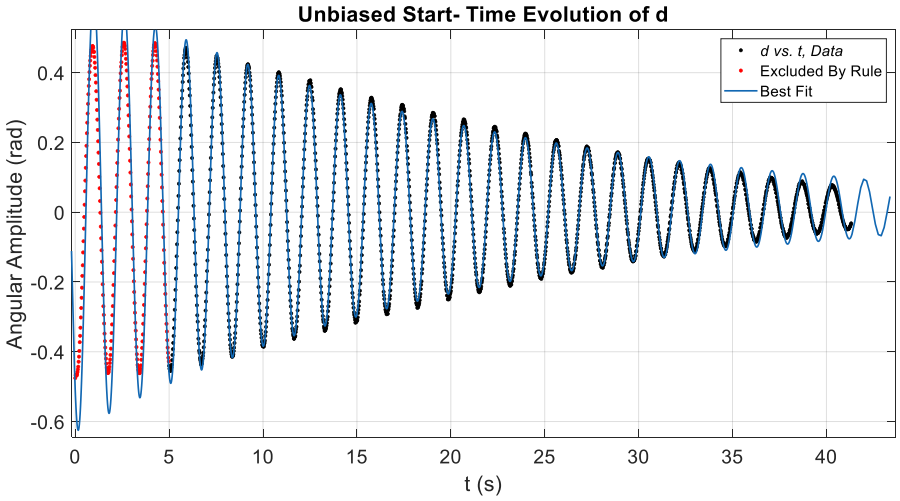

(a) Time evolution of d obtained from an unbiased start.

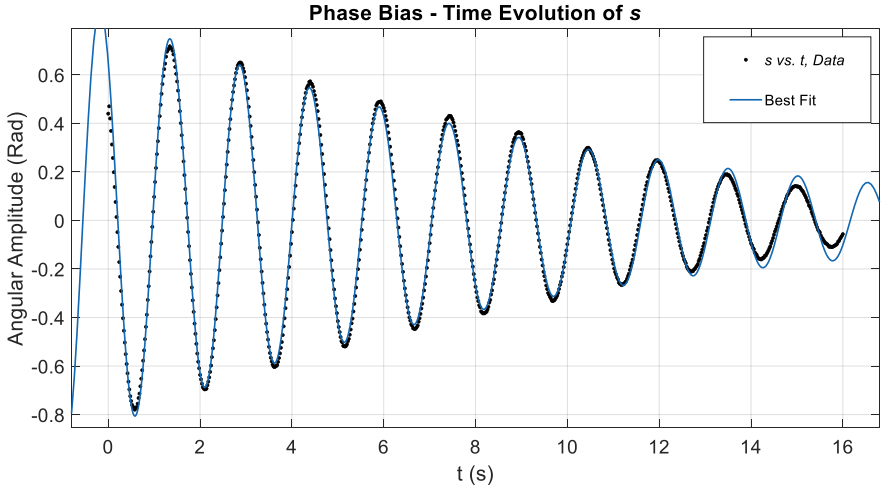

(b) Time evolution of s obtained from a biased start towards in-phase motion.

Figure 2.4: *Fits of the experimental data. Picture (a): Plot of d as a function of time, along with the best fit of the data. Here the pendulums were started with no particular bias towards phase or anti-phase motion, yet in about 10 seconds the anti-synchronous state was reached. The fitting region as been restricted, as it appears that virtually no dissipation occurs in the first 5 seconds. Picture (b): Plot of s and the best fit of the data as a function of time, obtained with a biased start towards phase motion ($A_d = B_d \approx 0$). While the angular frequency ω_s matches the predicted result, the decline in the amplitude of oscillations is much steeper than expected.*

Since we have data on both angular velocities and positions, we can swiftly com-

pute the energy of the system and confirm that the low angular velocity approximation discussed in Chapter 1 is valid (Fig. 2.5).

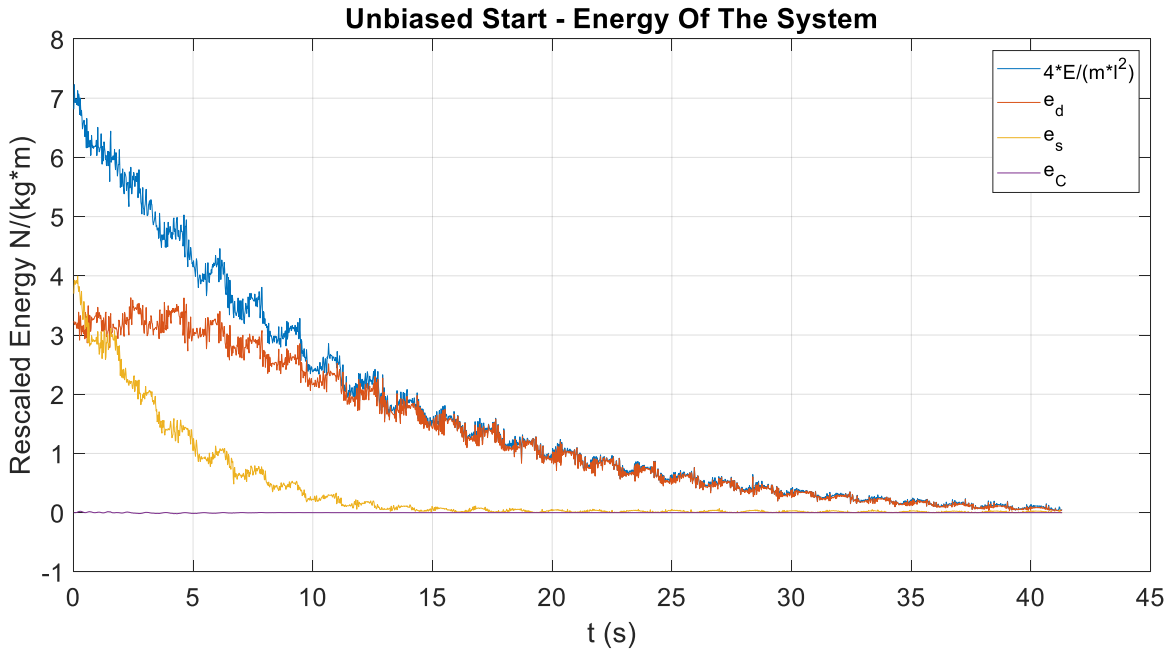

Figure 2.5: *The total rescaled system energy $4E/ml^2$ (blue), e_d (orange), e_s (yellow) and e_c (purple) plotted as a function of time. Note that e_c is negligible when compared to e_d and e_s, which is a confirmation of the validity of the model. At about 10 seconds, anti-phase synchronization occurs, hence $E_d \approx E$. The energy of the system is characterized by a clear exponential decay, which is correctly described by the equations of motion.*

The angular frequencies of phase and anti-phase motion are comparable with the values predicted by Eq. 1.11 and 1.12; the fit of data gathered from a setup with $l = 0.67\,\text{m}$ yield $\omega_d = 3.82\,\text{Hz} \approx \omega$ and $\omega_s = 4.14\,\text{Hz}$, which is slightly less than the expected value of $\omega/\sqrt{1-2a} \approx 4.22\,\text{Hz}$. On the other hand, the decay rate of s is much higher compared to d: while the latter has a value of $\gamma_d = 0.096\,\text{Hz}$, the former is twice as fast, with a value of $\gamma_s = 0.207\,\text{Hz} > \gamma_d/(1-2a)$. When the pendulums swing together the motion of the trolley is maximized and other effects not included in the model, such as friction on the cart, affect the evolution of s. The trolley should act purely as an ideal conveyor of energy, as a way for the pendulums to exchange momentum, and its dynamic should be described by the approximate form of Eq. 1.1, but this is not the case in the initial stages of motion (Fig. 2.6): the cart absorbs much more energy than what is predicted by the model (Eq. 1.18) and does not return it back with the oscillating masses, resulting in an ulterior dissipative effect and a much higher γ_s.

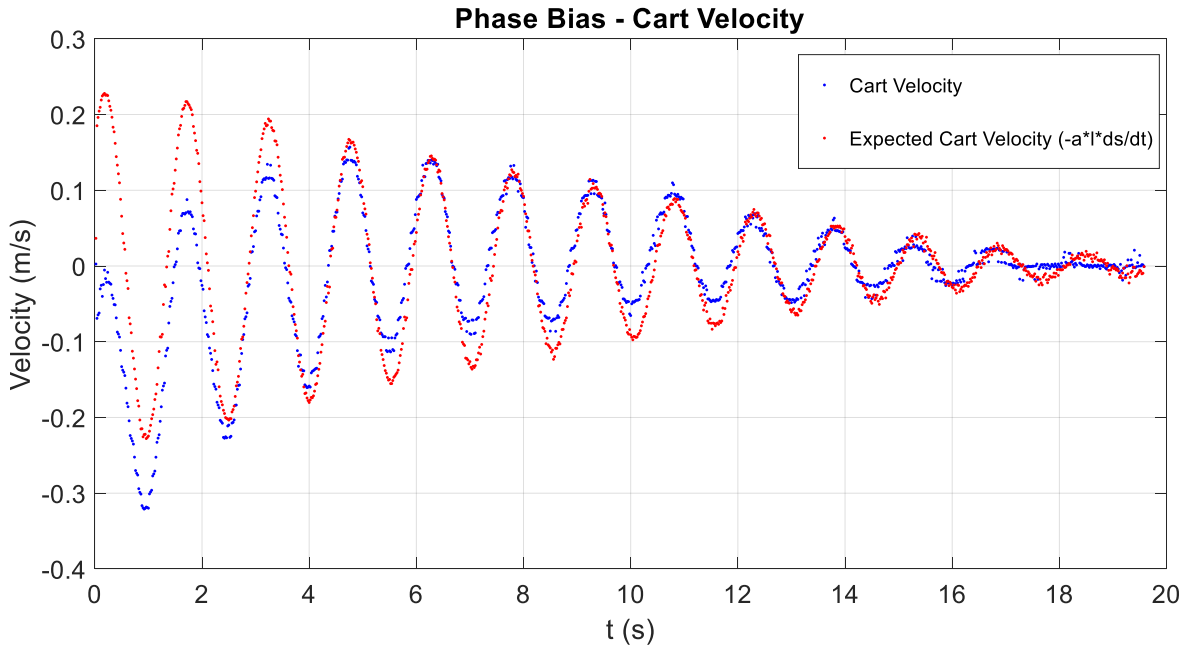

Figure 2.6: *Experimental data of the velocity of the cart, in blue the velocity acquired by tracking the center of the trolley, in red the expected value obtained through s, as described by Eq. 1.1. There is a discrepancy in the initial stages of motion not predicted by the model, which assumes an ideal cart; while the mismatch might seem negligible, it implies high differences energy wise, as the kinetic energy of the cart is proportional to the square of its velocity and its mass M.*

2.3 Metronomes: Experimental Data

Both synchronous states have been also observed in the setup built with metronomes, although one result was more likely than the other depending on the objects used as wheels: with an unbiased start, using spherical objects such as tennis balls favoured in-phase synchronization (as shown in the video of Ref. [14]) while using cylindrical objects, such as cans, favoured anti-phase motion [15]. The explanation of this effect is beyond the scope of the model, as the cart is assumed to be ideal and the objects used as wheels should make no difference; we assume that the system built with tennis balls is more energy efficient, since an inefficient cart favours anti-phase synchronization, as previously discussed. This conjecture is also compatible with Pantaleone's paper [9], in which friction on the trolley had to be artificially increased in order to observe anti-phase synchronization. Take into account that these rudimentary systems had to be employed in order not to further decrease the already low ratio between the oscillating mass m and the cart's mass M. The value of $a \approx 0.02$, has been fitted by reconstructing the dynamic

of the trolley and relating it to the dynamic of s using the approximate form of Eq. 1.1.

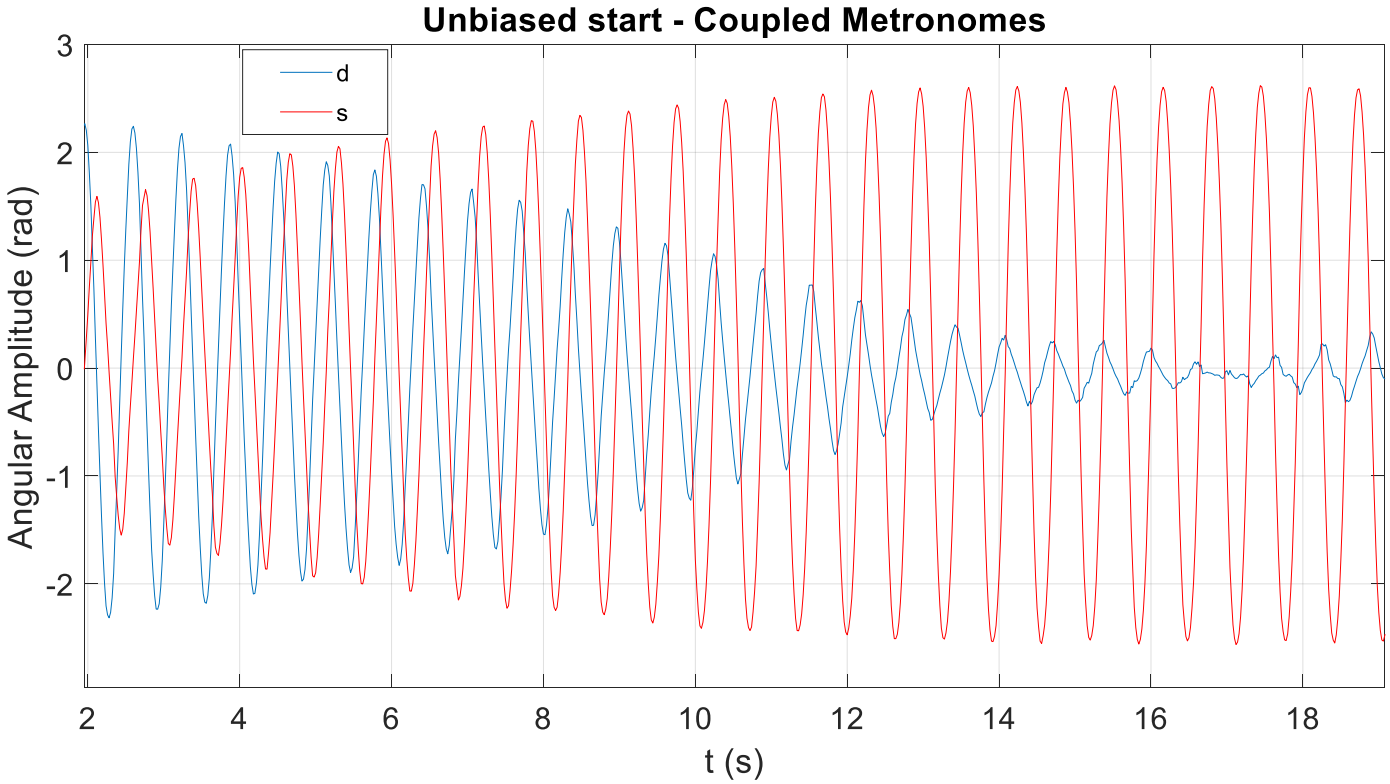

Figure 2.7: *Time evolution of d (blue) and s (red) obtained with an unbiased start. The system built using tennis balls as cart wheels, evolves towards an in-phase synchronized state. Synchronization is not perfect, as d is not identically null.*

In general synchronization is not perfect and only occurs at higher frequencies: after the oscillators reach the relative phase typical of a synchronous state ($2n\pi$ or $(2n+1)\pi$) there might be a transient time in which the phase changes; as long as this variation is contained and the metronomes reachieve their original synchronized state, we can claim that a weaker form of synchronization has occurred. This effect is caused by the intrinsic frequency difference $\Delta\omega$ between the two metronomes: despite being bought by the same manufacturer, their angular frequencies are not identical but the ratio $\Delta\omega/\omega$ decreases as ω increases. Therefore, an higher frequency implies a "stronger" form of synchronization, one where the transient time, in which the relative phase changes, is shorter and variations are smaller. A more formal definition of the quality of synchronization is provided in Chapter 3.
In order to obtain an estimate of the dissipation rate γ, the metronomes' springs have been unwound and the trajectories of the oscillating masses have been studied in the

single uncoupled case as well as the coupled one. When compared to the values estimated in the setup with pendulums, here the dissipation factors are much closer to the expected theoretical values (Fig. 2.8): $\gamma \approx \gamma_d = 0.24\,\text{Hz}$ and $\gamma_s = 0.26\,\text{Hz}$, which is quite close to the predicted value of $\gamma/(1-2a) = 0.25\,\text{Hz}$. This is a sign of a relatively efficient cart system.

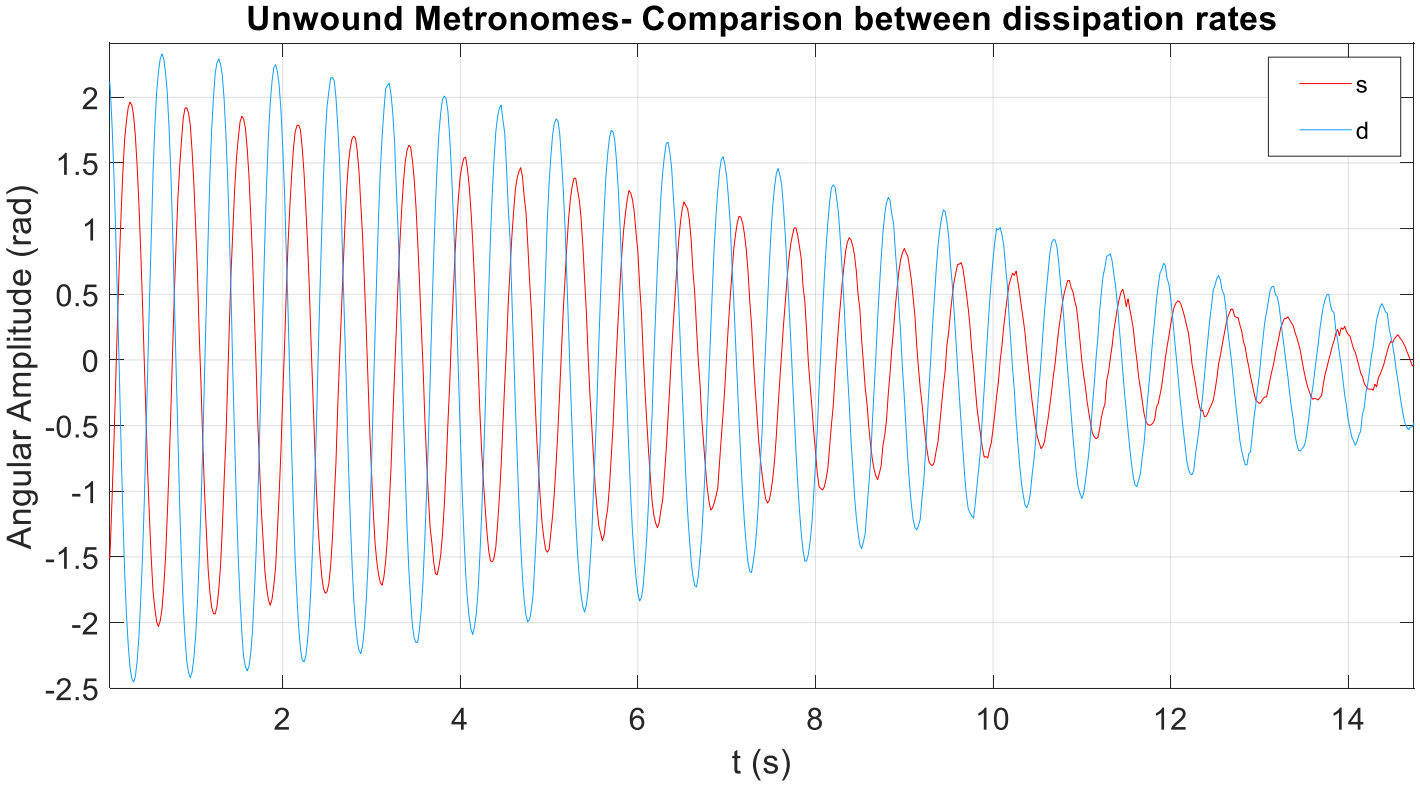

Figure 2.8: *Plot of d (blue) and s (red) as a function of time, obtained with metronomes whose springs have been unwound. The two sets of data have been acquired with different initial conditions, an anti-phase bias for the blue curve and a phase bias for the red one. The dissipation rates are close, as predicted by the model for a low value of a.*

The behaviour of the spring is correctly described by Dirac's delta (Eq. 1.19, 1.20) as shown in Fig. 2.9: the energy is injected seemingly instantly into the oscillating mass, affecting its velocity but not its position. In a neighbourhood of synchronous motion the dynamic is predicted by the model (Sect. 1.3): the time delay between the activation of the springs approaches 0 ($\epsilon_{n+1} < \epsilon_n$), which implies that eventually the springs get simultaneously triggered and the metronomes achieve a synchronous state, which, for a short duration, is virtually perfect.

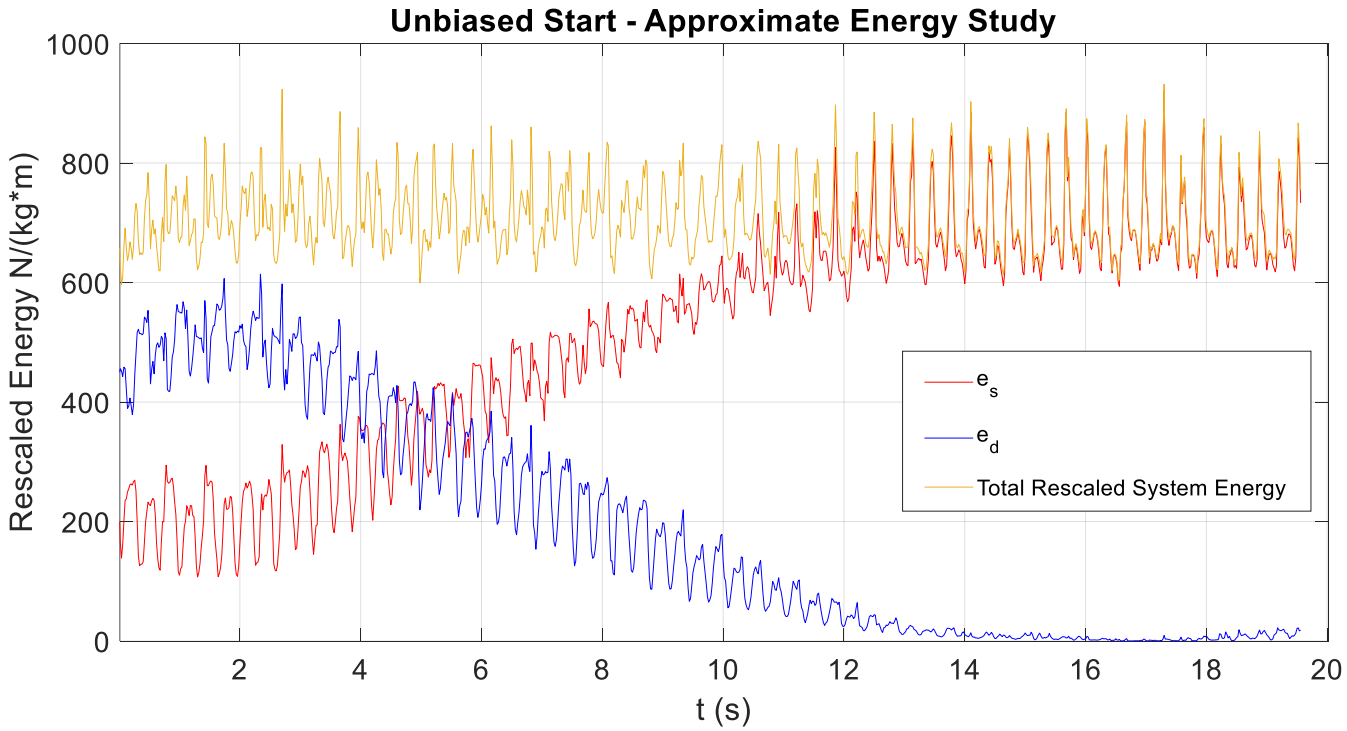

Figure 2.9: *Plot of the rescaled system energy $4E/(ml^2)$ (yellow), e_s (red) and e_d (blue). This graph does not provide a completely accurate picture of the energy of the system as it has been obtained using the small angle approximation, which is not valid, but the energy peaks caused by the two springs' action are clearly visible. As the pendulums reach in-phase motion ($\mathrm{sgn}(\dot{\theta}_1) = \mathrm{sgn}(\dot{\theta}_2)$) the peaks get closer in time, until perfect synchronization occurs and the effect of the springs is seen as an unison high energy spike. Since synchronization is not perfect, the peaks eventually decouple, while still remaining close.*

Chapter 3

Numerical Solutions

3.1 Equations of Motion and Synchronization Strength

Numerical analysis is a necessary tool to better understand the behaviour of coupled metronomes, as the equations which describe the dynamic are complex and no analytical solution can be found without employing approximations that do not accurately represent the physical reality of the setup. To facilitate the implementation of a Runge-Kutta algorithm, it is convenient to write the equations in the frame of reference of the trolley, which is not an inertial system and therefore fictitious forces should be taken into account (as shown in [9]). The equations which describe the angular position of the oscillating mass of each metronome are

$$\ddot{\theta_1} + \gamma\dot{\theta_1} + \omega_1^2 \sin\theta_1 + \cos\theta_1 \frac{\ddot{X}}{l} = K' \operatorname{sgn}(\dot{\theta_1})\delta(\theta_1) \tag{3.1}$$

$$\ddot{\theta_2} + \gamma\dot{\theta_2} + \omega_2^2 \sin\theta_2 + \cos\theta_2 \frac{\ddot{X}}{l} = K' \operatorname{sgn}(\dot{\theta_2})\delta(\theta_2) \tag{3.2}$$

By recalling Eq. 1.1 we can substitute $\ddot{X}/l$ with $a(\sin\theta_1\dot{\theta_1}^2 - \cos\theta_1\ddot{\theta_1} + \sin\theta_2\dot{\theta_2}^2 - \cos\theta_2\ddot{\theta_2})$. These equations have been thoroughly studied by implementing a Runge-Kutta 4 integration method. This framework allows to introduce differences in the angular frequencies of the metronomes (ω_1, ω_2) in order to study the "weaker" form of synchronization which was observed experimentally. The strength of synchronization S at a given time t and a given time interval Δt can be defined as

$$S(t, \Delta t) = \frac{\max(|s|) - \max(|d|)}{2A_\omega} \tag{3.3}$$

where $\max(|s|)$ and $\max(|d|)$ respectively are the maximum values of $|\theta_1 + \theta_2|$ and $|\theta_1 - \theta_2|$ in the time interval $[t - \frac{\Delta t}{2}, t + \frac{\Delta t}{2}]$ and A_ω is the amplitude of oscillations computed at the nominal frequency ω of the metronomes (Sect. 1.4). Since the amplitude of oscillations

for s and d in perfectly synchronized states is $2A_\omega$, an absolute value of S near 1 defines a strong synchronization, while $S \approx 0$ represents the lack of synchronized motion. Any value in between is a measure of the quality of synchronization, while the sign of S denotes the tendency towards an in-phase (positive S) or an anti-phase (negative S) state. Notice that the choice of t and Δt deeply influence the value of S (Fig. 3.4); the fact that synchronization does not occur in the chosen time interval does not imply that eventually the system will not evolve towards synchronized motion.

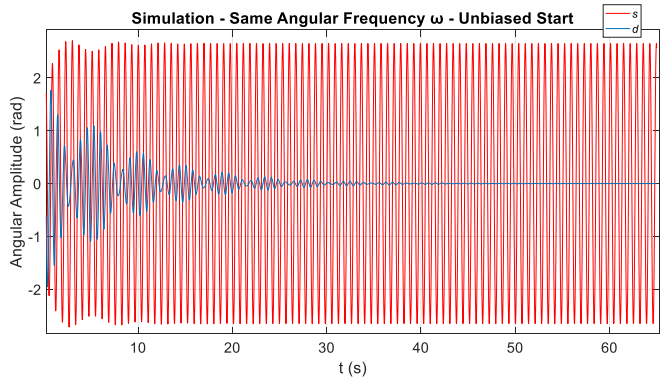

(a) Simulation of the system with $\omega_1 = \omega_2 = \omega$.

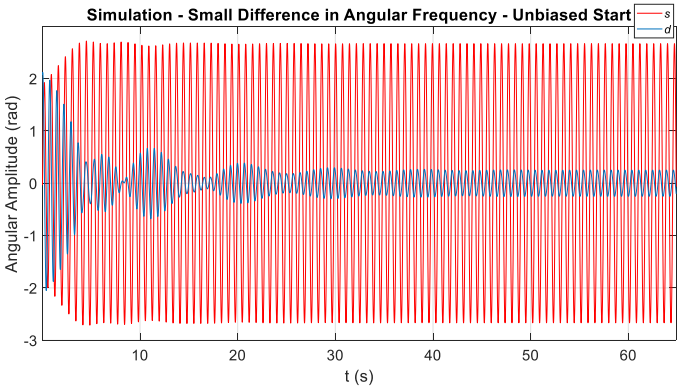

(b) Simulation of the system with $\frac{\omega_1 - \omega_2}{\omega} \approx 0.03$

Figure 3.1: *Simulated time evolution of s and d, represented respectively by the red and the blue curve. In picture (a) the oscillators have the same angular frequency so a wise choice of t and Δt provides an accurate evaluation of $S \approx 1$. In picture (b) the two frequencies have been set to different values, yet close to the nominal frequency $\omega = 10.05\,\frac{\text{rad}}{\text{s}}$, to provide a more accurate depiction of the experimental setup. In the final stages of motion $S \approx 0.9$, hence synchronization is not perfect*

3.2 Results of Simulations

In Section 1.3 it is shown that in principle both in-phase and anti-phase motion provide a stable solution to the system of equations, although the final synchronous state depends on the parameters of the simulation and the initial conditions. For instance an higher value of a favours anti-phase synchronization, as γ_s is proportional to $1/(1-2a)$. On the contrary, an higher frequency implies higher angular velocities as well as cart velocity, since they are bound by the conservation of momentum, and values of K (Eq. 1.28, A scales with ω) which means that any effect which favours in-phase synchronization will be further enhanced. The springs by acting on the oscillating masses indirectly affect the dynamic of the cart, pushing it in the opposite direction: when the trolley receives the boost from the first spring, it skews the oscillations towards in-phase motion, as a fictitious force acts on both oscillating masses, delaying the second boost if it happened to be in the opposite direction ($\operatorname{sgn}(\dot{\theta}_1) = -\operatorname{sgn}(\dot{\theta}_2)$) while anticipating it in the other case ($\operatorname{sgn}(\dot{\theta}_1) = \operatorname{sgn}(\dot{\theta}_2)$), reducing the range of conditions which fall in the neighborhood of anti-phase motion, as the values ϵ_n studied in Sect. 1.3 are affected. These observations are backed both by experimental data (Sect. 2.3) and simulations (Fig. 3.2).

It is possible to run the experiment, as well as the simulations, with special initial conditions characterized by any initial positions ($-A_\omega \leq \theta_1, \theta_2 \leq A_\omega$) and no initial velocities ($\dot{\theta}_1 = \dot{\theta}_2 = 0$); when these conditions are met, the two bisectors of the configuration space identify the starts with a strong bias towards in-phase ($\theta_1 = \theta_2$) and anti-phase ($\theta_1 = -\theta_2$) motion. Simulations conducted with $a = 0.02$ show that with lower frequencies ($\omega \approx 3\frac{\text{rad}}{\text{s}}$) there is an even amount of in-phase and anti-phase final synchronous states, where the former occupy the first and third sectors of the plane while the latter populate the second and the fourth sectors. As frequencies get higher, in-phase synchronization becomes more likely, and the initial conditions which lead to anti-phase synchronicity get restricted to narrower regions along the bisector $\theta_1 = -\theta_2$. Fig. 3.3 shows this effect.

As one would expect, an increase in the frequency difference $\omega_1 - \omega_2$ causes in-phase synchronization to become less likely and of the weaker kind ($S < 1$) whenever it does occur. Fig. 3.4 shows how the introduction of different frequencies in the model can produce results which better resemble experimental data.

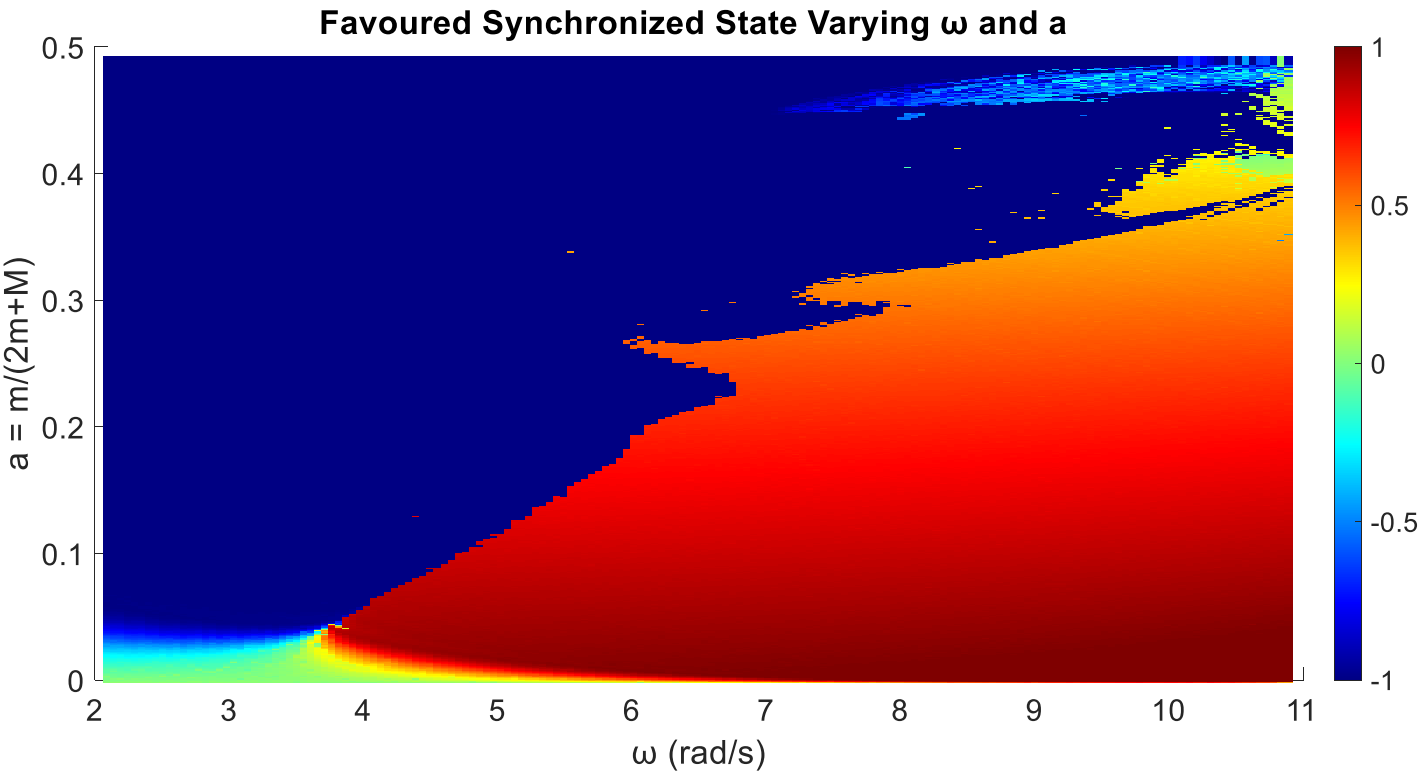

Figure 3.2: *Results of many simulations of identical metronomes ($\omega_1 = \omega_2 = \omega$) run with different values of a and ω. The same unbiased initial conditions produced different final states depending on the values of the parameters. The heatmap represents the value of $S(t = 47.5s, \Delta t = 5s)$; perfectly anti-synchronized motion ($S = -1$) is represented by the color dark blue, while dark red stands for perfect in-phase synchronization ($S = 1$). Colors of a lighter shade represent weaker (or lack of) synchronization.*

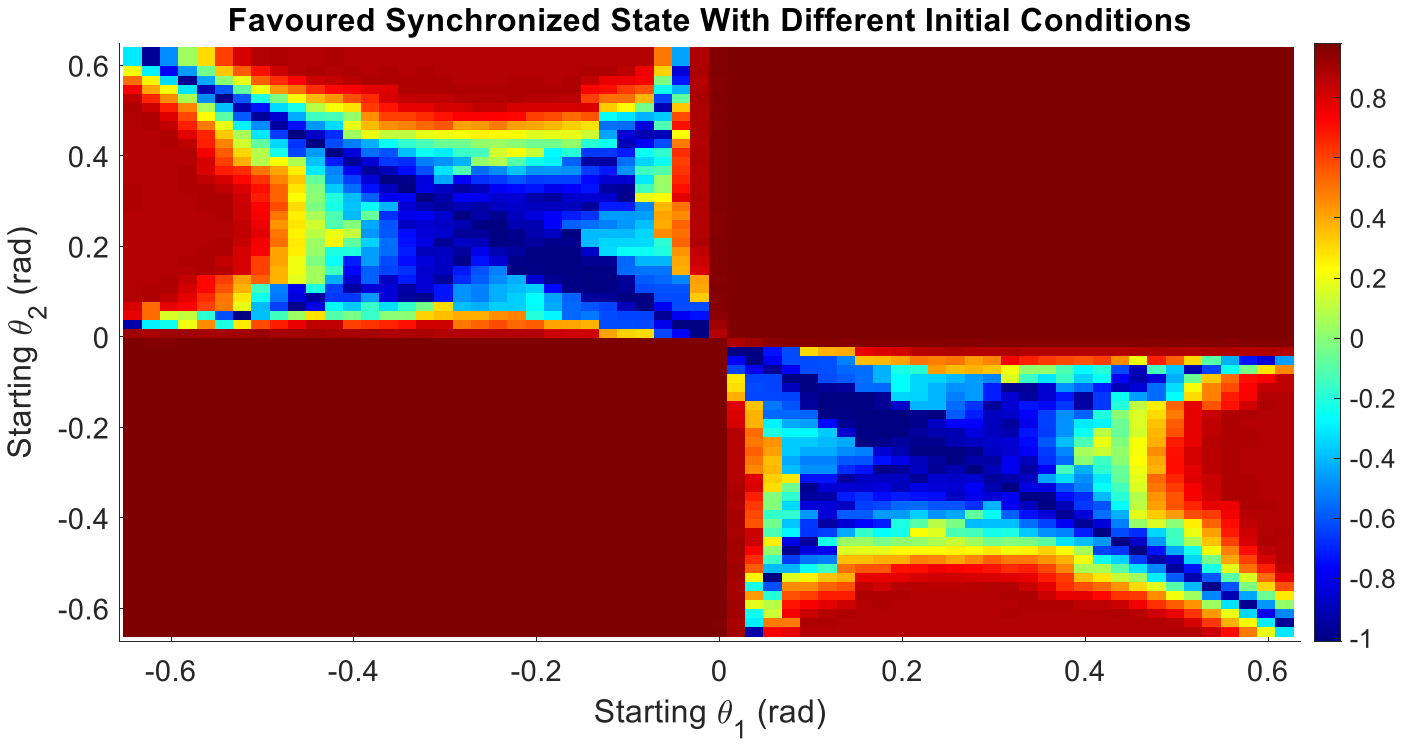

Figure 3.3: *Results of many simulations of identical metronomes ($\omega_1 = \omega_2 = 2\pi \frac{\text{rad}}{\text{s}}$) run with different initial conditions, defined by null velocities ($\dot{\theta}_1 = \dot{\theta}_2 = 0$) and varying initial positions. The heatmap represents the value of $S(t = 47.5s, \Delta t = 5s)$; perfectly anti-synchronized motion ($S = -1$) is represented by the color dark blue, while dark red stands for perfect in-phase synchronization ($S = 1$). Colors of a lighter shade represent weaker (or lack of) synchronization.*

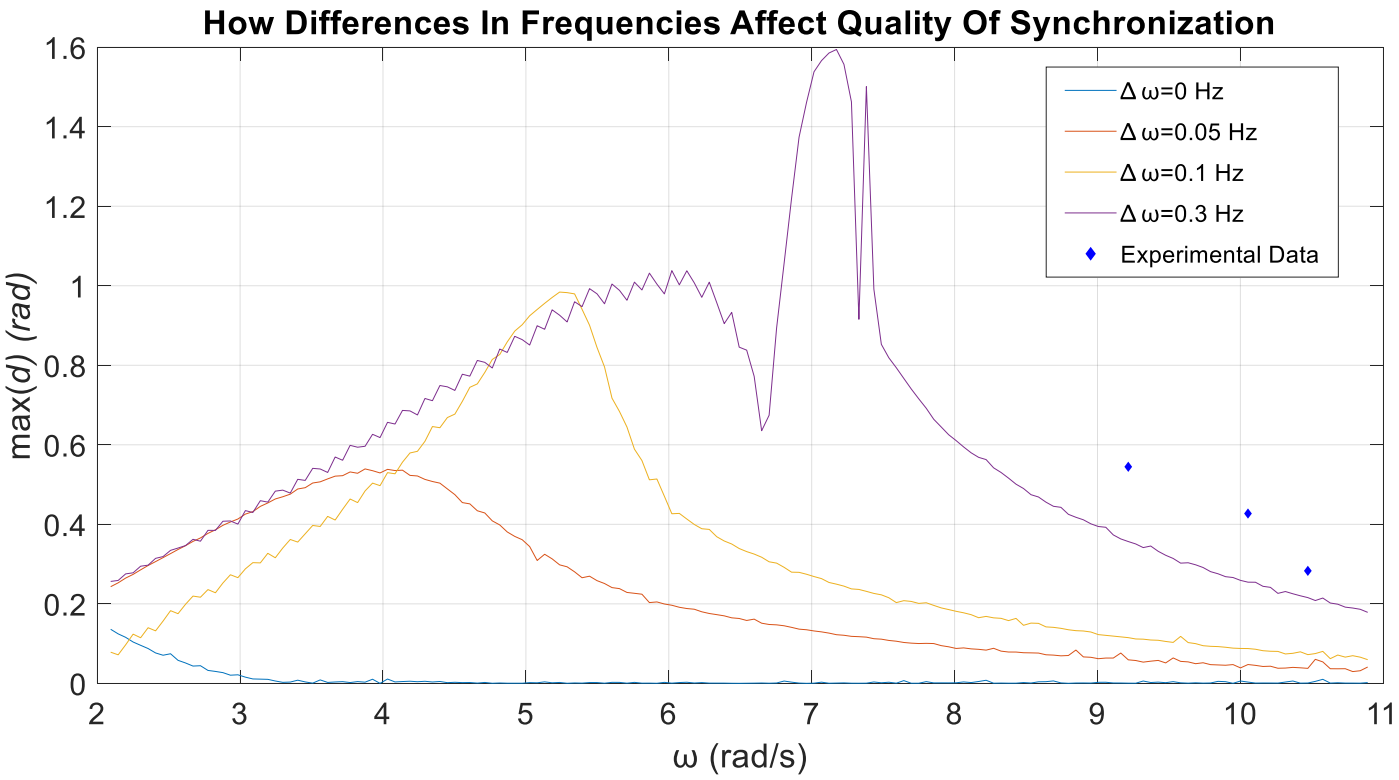

Figure 3.4: $\max(|d|)$ *evaluated in the time interval* $[45\,\mathrm{s}, 50\,\mathrm{s}]$ *for different nominal frequencies. The various curves are results of simulations of systems characterized by an intrinsic frequency difference of magnitude* $\Delta\omega = \omega_1 - \omega_2$*: 0 (blue), 0.05 (orange), 0.1 (yellow) and 0.3 (purple) Hz. The blue diamonds represent data acquired from the metronomes used in the experiment; their placement somewhat resembles the trend of the other curves. Despite a biased start towards in-phase motion, differences in oscillator frequencies deeply affect the quality of synchronization.*

Conclusions

The synchronization phenomenon is strictly correlated to the presence of dissipation and external forcing that allow the system to relax toward a stationary state. In the performed experiment the possibility of writing the relevant physical quantities as a function of the difference d and the sum s of the angular positions of the oscillators provided useful insights on synchronization, linking the phenomenon to the change of energy. Both in-phase and anti-phase motion have been observed, confirming that all synchronous states constitute stable solutions of the systems. However, the assumptions employed did not always lead to accurate predictions of all the parameters which characterize our setup; while there is a qualitative good accordance between experimental data and theoretical values for ω_d, ω_s and γ_d, the obtained value for γ_s is generally higher than the expected one of $\gamma_d/(1-2a)$. This mismatch is probably caused by approximations which do not perfectly describe the reality of the apparatus, namely the assumption of an ideal trolley; we believe that the model could convincingly describe the dynamic of a more professional setup, one where the cart can truly be considered frictionless. An ideal setup would be built using lighter trolleys with better air cushions; perhaps these could also be employed in the system of coupled metronomes, since they would increase the effectiveness of coupling, which can be further improved by acquiring more professional metronomes, with a lower intrinsic frequency difference $\Delta\omega$.
Numerical analysis has proven the robustness of the models, which can be tuned to reproduce the imperfections of real-world oscillators.

Bibliography

[1] F. Orsucci, R. Petrosino, G. Paoloni et al., *Prosody and Synchronization in Cognitive Neuroscience*, EPJ Nonlinear Biomed. Phys. **1**, 6 (2013).

[2] K. Stein, A. Timmermann, and N. Schneider, *Phase Synchronization of the El Niño-Southern Oscillation with the Annual Cycle*, Phys. Rev. Lett. **107**, 128501 (2011).

[3] J. Foster, *From Simplistic to Complex Systems in Economics*, Cambridge Journal of Economics **29**, 6, p. 873 (2005).

[4] X. H. Zhang, H. W. Zhang, B. Chen et al., *Water Resources Planning Based on Complex System Dynamics: A Case Study of Tianjin City*, Communications in Nonlinear Science and Numerical Simulation **13**, 10, p. 2328 (2008).

[5] E. E. Verheijck, R. Wilders, R. W. Joyner et al., *Pacemaker Synchronization of Electrically Coupled Rabbit Sinoatrial Node Cells*, Journal of General Physiology, **111**, 1, p. 95 (1998).

[6] A. Tyrrell, G. Auer, and C. Bettstetter, *Fireflies as Role Models for Synchronization in Ad Hoc Networks*, Proceedings of 1st Bio-Inspired Models of Network, Information and Computing Systems conference. (2006).

[7] F. A. Rodrigues, T. K. DM. Peron, P. Ji, and J. Kurths, *The Kuramoto Model in Complex Networks*, Physics Reports **610**, p. 1 (2016).

[8] C. Huygens, *Horologium Oscillatorium* (F. Muguet, Parisii, 1673). English translation: Richard J. Blackwell, *The Pendulum Clock* (Iowa State University Press, Ames, 1986).

[9] J. Pantaleone, *Synchronization of Metronomes*, American Journal of Physics **70**, p. 992 (2002).

[10] N.V. Kuznetsov, G.A. Leonov, H. Nijmeijer, A. Pogromsky *Synchronization of two metronomes*, Proceedings of the 3rd IFAC Workshop (PSYCO'07), IFAC Proceedings Volumes, **40**, 14, p. 49 (2007).

[11] D. Brown, W. Christian, R. M. Hanson, *Tracker: Video Analysis and Modeling Tool*, 2023. Homepage: https://physlets.org/tracker/

[12] Pendulums anti-phase synchronization [video] https://youtu.be/mZX9nVkjEbQ

[13] Pendulums in-phase motion [video] https://youtu.be/gak3cgSGy_4

[14] Metronomes in-phase synchronization [video] https://youtu.be/JRk5oCsKobo

[15] Metronomes anti-phase synchronization [video] https://youtu.be/JRk5oCsKobo